

Supporting Information

for

Rationalizing Fluorescence Quenching in *meso*- BODIPY Dyes

Antonio Prlj,^{1†} Alberto Fabrizio,^{1†} Clemence Corminboeuf^{†}*

¹Institut des Sciences et Ingénierie Chimiques, Ecole Polytechnique Fédérale de Lausanne, CH-1015

Lausanne, Switzerland

[†]Authors contributed equally

Contents

1. Photophysical data
2. Optimized structures (xyz)
3. Formyl- and hydroxymethyl-BODIPY
4. Excited state dynamics
5. Solvent effects
6. References

1. Photophysical data

The relevant photophysical data for *meso*-vinyl-BODIPY (**1**) and *meso*-ethyl-BODIPY (**2**) are reported in Table S1. Table S2 demonstrates the weak basis set dependence of the excitation energies, which is characteristic for cyanine dyes. The large excited state relaxation (and Stokes shift) of **1** can be explained by the partial delocalization of the excitation to the vinyl substituent (see density differences in Figure S1).

Table S1. Photophysical data for **1** and **2** computed at the ADC(2)/def2-SVP level. Oscillator strengths are reported in parentheses.

	1	2
S ₁ (vertical)	2.69 eV (0.445)	2.79 eV (0.478)
S ₂ (vertical)	3.65 eV (0.176)	3.82 eV (0.186)
S ₃ (vertical)	3.82 eV (0.023)	3.98 eV (0.035)
S ₁ (adiabatic)	2.30 eV	2.65 eV
S ₁ (emission)	1.17 eV (0.114)	2.32 eV (0.290)
S ₀ /S ₁ MECP (relative to S ₀ min.)	2.39 eV	2.76 eV

Table S2. Excitation energies basis set dependence at the ADC(2) level.

basis set	1		2	
	S ₁ (vertical)	S ₂ (vertical)	S ₁ (vertical)	S ₂ (vertical)
def2-SVP	2.69 eV	3.65 eV	2.79 eV	3.82 eV
def2-TZVP	2.63 eV	3.54 eV	2.73 eV	3.71 eV
def2-TZVPD	2.61 eV	3.53 eV	2.72 eV	3.70 eV

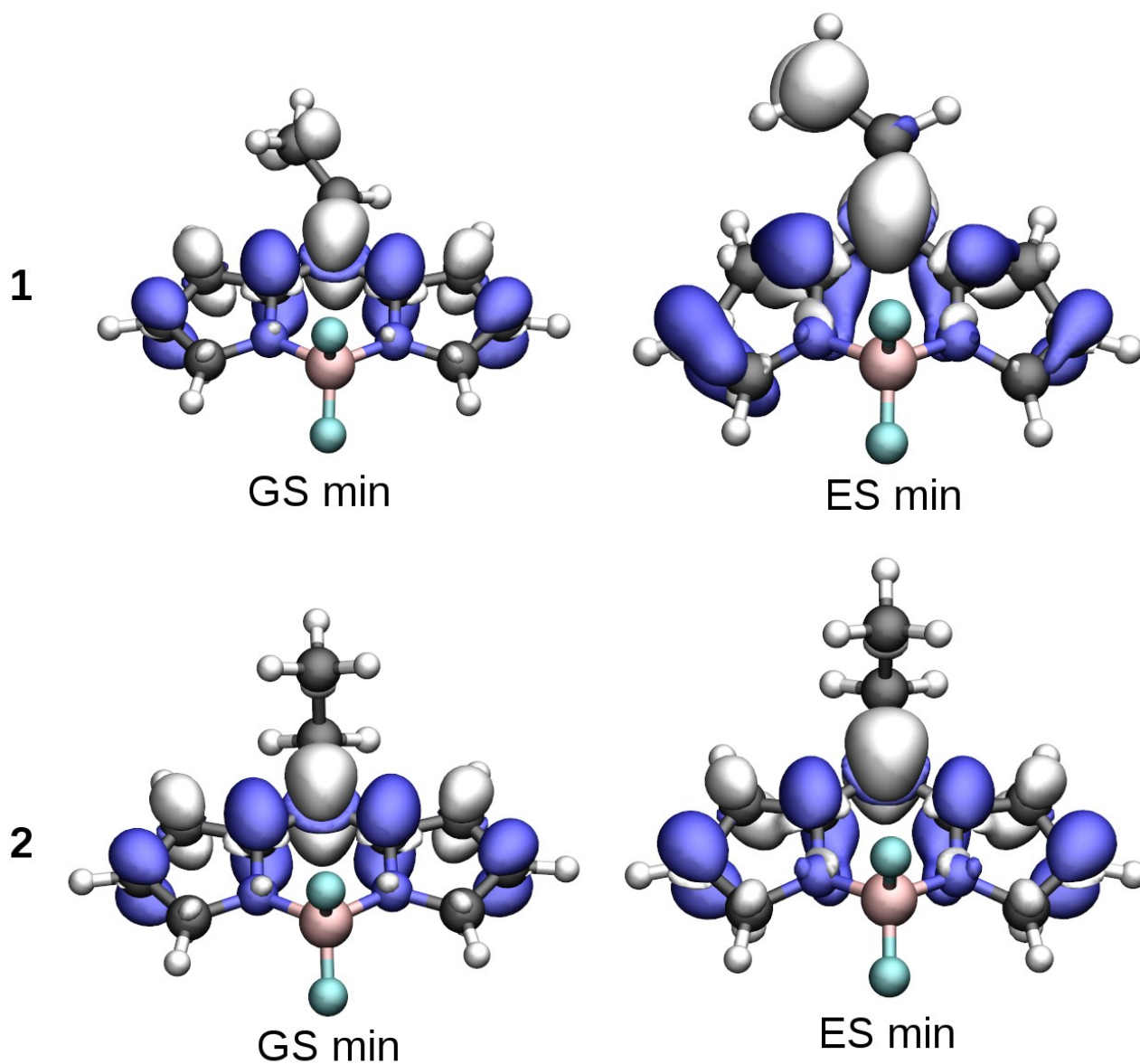


Figure S1. Density differences between the S_1 and S_0 states at the optimized ground state (GS) and the excited state (ES) geometries of **1** and **2**. The density gain/depletion is shown in white/blue (isovalue 0.0025). ADC(2)/def2-SVP level of theory was used.

2. Optimized structures (xyz)

meso-vinyl-BODIPY: S₀ minimum

25

N	0.172098	0.518675	1.179414
B	-1.260339	1.161176	1.213604
N	-1.791732	0.972288	-0.251189
C	-1.001524	0.797181	-1.370727
C	-1.859832	0.741454	-2.514291
C	0.380100	0.554382	-1.237415
C	1.242811	0.448830	-2.419512
C	0.941784	0.374948	0.041674
C	2.257304	-0.013334	0.440516
C	2.243440	-0.102051	1.829165
C	-3.159375	0.907235	-2.046096
C	0.937830	0.243942	2.250848
C	-3.076865	1.047933	-0.640965
H	0.525840	0.311957	3.257180
F	-1.154515	2.508230	1.505735
F	-2.070991	0.486729	2.102171
H	3.093612	-0.213722	-0.226956
H	3.067706	-0.386619	2.480438
H	-4.076412	0.905042	-2.632215
H	-3.869326	1.186295	0.093755
H	-1.541506	0.548748	-3.536290
C	1.141481	1.267472	-3.486699
H	2.034958	-0.305342	-2.390256
H	0.403135	2.070987	-3.517595
H	1.824575	1.167518	-4.332751

meso-vinyl-BODIPY: S₁ minimum

25

N	0.223458	0.719152	1.138982
B	-1.006631	1.686530	1.048636
N	-1.675820	1.191593	-0.292637
C	-0.918997	0.769172	-1.381744
C	-1.781130	0.219626	-2.351522
C	0.551005	0.859837	-1.285909
C	1.423955	1.207463	-2.332532
C	0.966155	0.351855	0.020543
C	1.980973	-0.537506	0.421302
C	1.858659	-0.668866	1.816573

C	-3.081829	0.366044	-1.843687
C	0.750394	0.115585	2.220646
C	-2.969552	0.955583	-0.552326
H	0.323425	0.272216	3.210434
F	-0.591598	2.993202	0.919269
F	-1.866235	1.471907	2.102056
H	2.705214	-1.015713	-0.236448
H	2.490717	-1.261228	2.477279
H	-4.014553	0.089490	-2.334559
H	-3.740817	1.201451	0.176632
H	-1.475235	-0.216859	-3.300376
C	1.026752	1.629867	-3.579145
H	2.494989	1.153500	-2.106007
H	-0.032576	1.732221	-3.830021
H	1.763534	1.913833	-4.333899

meso-vinyl-BODIPY: S₁/S₀MECP

25

N	-0.754114	-0.123829	1.304542
B	-2.007847	0.821028	1.094799
N	-2.542785	0.297737	-0.294687
C	-1.679922	-0.119430	-1.304924
C	-2.442489	-0.717547	-2.332369
C	-0.244772	0.146136	-1.077692
C	0.594857	1.012444	-1.778330
C	0.014354	-0.526393	0.216880
C	0.876904	-1.567030	0.631703
C	0.669512	-1.726730	2.003925
C	-3.782684	-0.583652	-1.952449
C	-0.382923	-0.839065	2.376771
C	-3.802503	0.026043	-0.667653
H	-0.876902	-0.720145	3.340041
F	-1.613131	2.134737	0.997524
F	-2.941192	0.579797	2.076098
H	1.605550	-2.067641	-0.001488
H	1.205646	-2.391733	2.681769
H	-4.662849	-0.873961	-2.525512
H	-4.645293	0.262505	-0.019053
H	-2.043542	-1.125593	-3.259963
C	0.247498	1.684309	-2.932002
H	1.609688	1.138005	-1.380983
H	-0.745027	1.574947	-3.377476
H	0.952305	2.367384	-3.407901

meso-ethyl-BODIPY: S₀ minimum

27

N	0.158586	0.579933	1.019824
B	-1.302291	1.152697	1.079143
N	-1.882431	0.866651	-0.351720
C	-1.125386	0.644072	-1.487331
C	-2.012418	0.597720	-2.607379
C	0.254379	0.394766	-1.396249
C	1.074028	0.245192	-2.645630
C	0.880892	0.362317	-0.139037
C	2.212856	-0.000346	0.232043
C	2.260011	0.015473	1.622269
C	-3.295655	0.803854	-2.111336
C	0.969766	0.382438	2.073580
C	-3.173812	0.969385	-0.711006
F	-1.256632	2.517806	1.295233
F	-2.039109	0.488870	2.037280
H	3.113362	-0.218585	2.255971
H	-4.225652	0.825178	-2.676315
H	0.464688	-0.225586	-3.430062
H	1.918285	-0.431433	-2.451431
C	1.594220	1.602740	-3.132247
H	0.757568	2.281005	-3.349276
H	2.191304	1.481166	-4.047426
H	2.224641	2.071854	-2.364345
H	3.020441	-0.253233	-0.452700
H	0.598078	0.510127	3.089797
H	-3.943381	1.154694	0.037689
H	-1.726222	0.419357	-3.642435

meso-ethyl-BODIPY: S₁ minimum

27

N	0.156566	0.667318	0.991999
B	-1.171661	1.484596	0.955301
N	-1.839189	0.950287	-0.349440
C	-1.119777	0.611414	-1.510394
C	-2.039361	0.313579	-2.531237
C	0.320590	0.511694	-1.470079
C	1.147054	0.454328	-2.711697
C	0.893488	0.325971	-0.157193
C	2.098362	-0.273126	0.249927
C	2.076635	-0.291034	1.665407
C	-3.327778	0.475254	-1.967182
C	0.853575	0.292279	2.079513

C	-3.154782	0.860621	-0.614717
F	-0.899115	2.835808	0.834917
F	-1.951712	1.186333	2.052980
H	2.856638	-0.667806	2.326408
H	-4.283932	0.344573	-2.473128
H	0.560733	0.002708	-3.528554
H	2.015481	-0.205191	-2.550691
C	1.627910	1.848747	-3.130646
H	0.769731	2.509869	-3.318722
H	2.236343	1.800206	-4.046333
H	2.235689	2.300353	-2.333405
H	2.875283	-0.665946	-0.403045
H	0.465219	0.475260	3.080546
H	-3.894470	1.093426	0.150156
H	-1.797405	-0.003406	-3.543789

meso-ethyl-BODIPY: S₁/S₀MECP

27

N	0.508562	-0.217963	0.474457
B	-0.124158	1.161410	0.902703
N	-0.710001	1.681832	-0.469013
C	-0.061818	1.422545	-1.665056
C	-0.893487	1.817212	-2.735609
C	1.286828	0.824388	-1.584884
C	2.562471	1.598937	-1.653620
C	1.124241	-0.389860	-0.755805
C	1.478125	-1.746232	-0.903378
C	1.114714	-2.377381	0.293680
C	-2.037918	2.373837	-2.154203
C	0.500803	-1.399742	1.120403
C	-1.895069	2.258863	-0.744362
F	0.862402	2.016449	1.354904
F	-1.141922	0.957651	1.805319
H	1.275999	-3.420902	0.558464
H	-2.884905	2.818293	-2.673140
H	3.343183	0.953864	-2.097599
H	2.892649	1.803303	-0.615312
C	2.441714	2.907552	-2.424458
H	2.151529	2.730285	-3.469837
H	3.398156	3.448497	-2.422584
H	1.682196	3.561909	-1.972169
H	1.988688	-2.179490	-1.762111
H	0.073361	-1.493005	2.119458
H	-2.572613	2.562440	0.051509
H	-0.645857	1.734448	-3.792458

3. Formyl- and hydroxymethyl-BODIPY

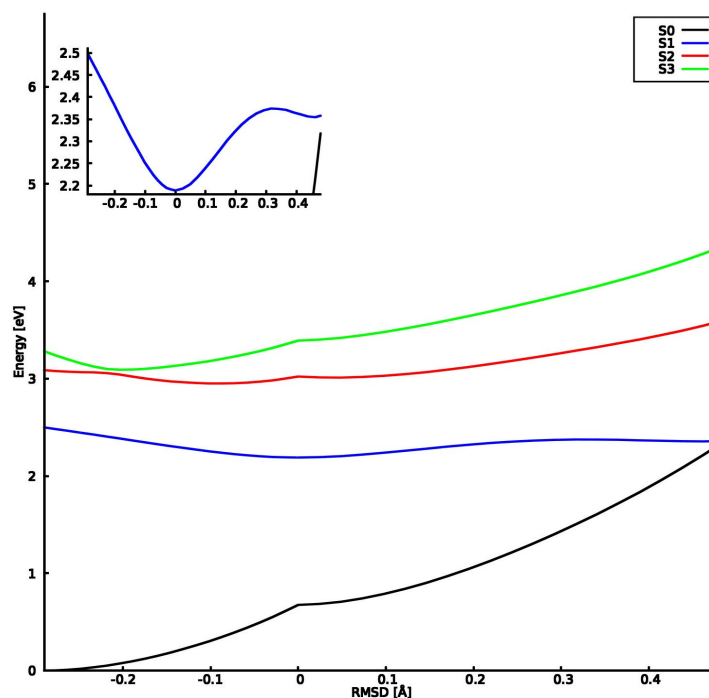


Figure S2. Energy profile (in eV) of *meso*-formyl-BODIPY. The ground and excited state minima and minimal energy crossing point (MECP) structures were optimized and connected by linear interpolation of internal coordinates. A zoom into the S_1 landscape is shown in the smaller graphs. The ADC(2)/MP2 levels were used with def2-SVP basis set.

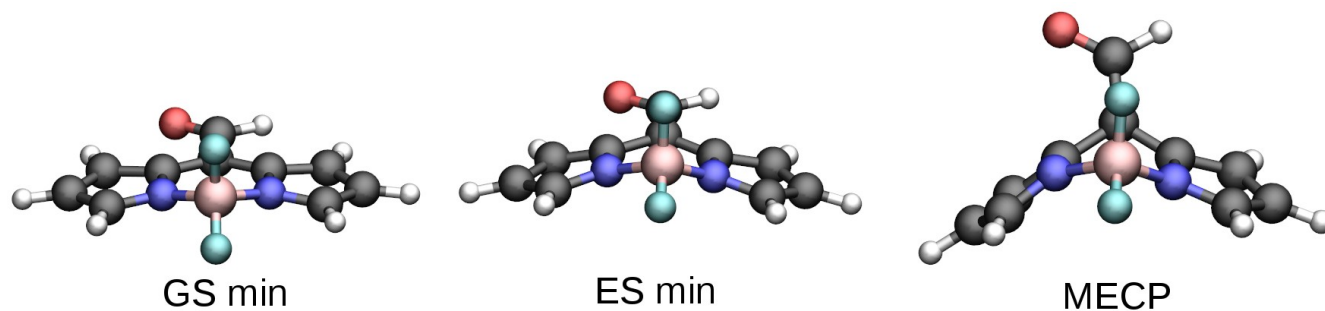


Figure S3. Structures of ground (GS) and excited state (ES) minima as well as S_1/S_0 minimal energy crossing point (MECP) of *meso*-formyl-BODIPY. The ADC(2)/MP2 levels were used with def2-SVP basis set.

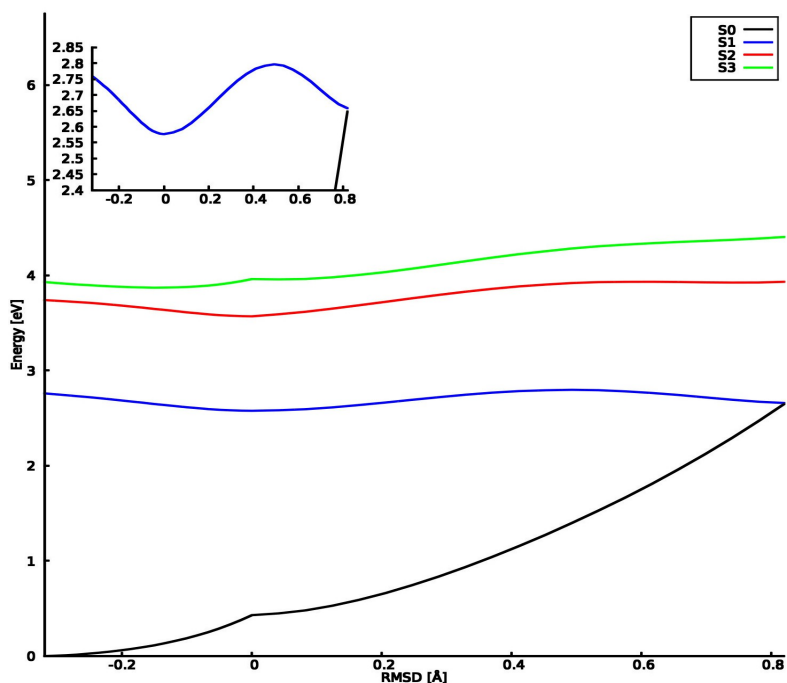


Figure S4. Energy profile (in eV) of *meso*-hydroxymethyl-BODIPY. The ground and excited state minima and minimal energy crossing point (MECP) structures were optimized and connected by linear interpolation of internal coordinates. A zoom into the S_1 landscape is shown in smaller graphs. The ADC(2)/MP2 levels were used with def2-SVP basis set.

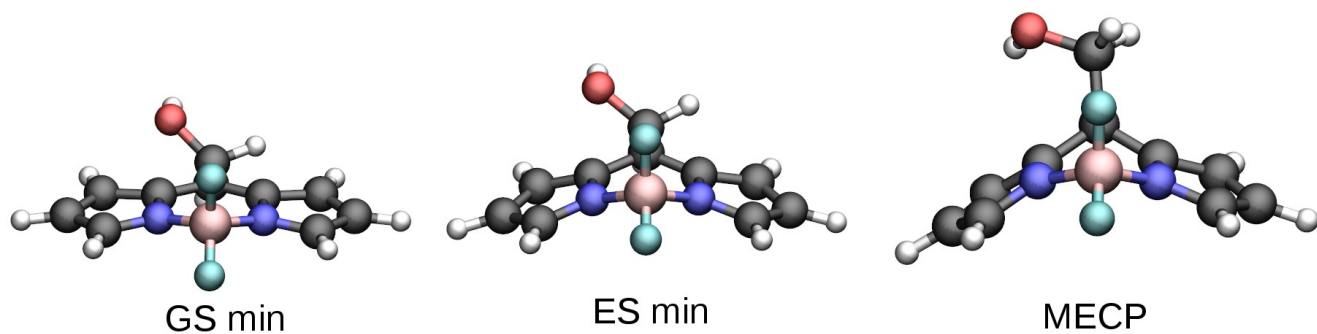


Figure S5. Structures of ground (GS) and excited state (ES) minima as well as S_1/S_0 minimal energy crossing point (MECP) of *meso*-hydroxymethyl-BODIPY. The ADC(2)/MP2 levels were used with def2-SVP basis set.

4. Excited State Dynamics

50 trajectories of both **1** and **2** were computed in the first excited singlet state. Due to the limitations of the ADC(2) method (single reference method) and the lack of coupling between the excited states and the ground state (MP2 level) all the trajectories that reach the S_1/S_0 crossing were terminated. To estimate the lower bound for the S_1 state lifetime we assume that the system switches to the ground state after reaching the crossing. By using this very approximate assumption we plot the decay of S_1 population as a function of time for compound **1** (figure S6). We set a delay time of 305 fs (no change in population) and fit an exponential function to the subsequent decay curve. The computed exponential decay constant of 218 fs added to the delay time of 305 fs gives a total decay time of 523 fs.

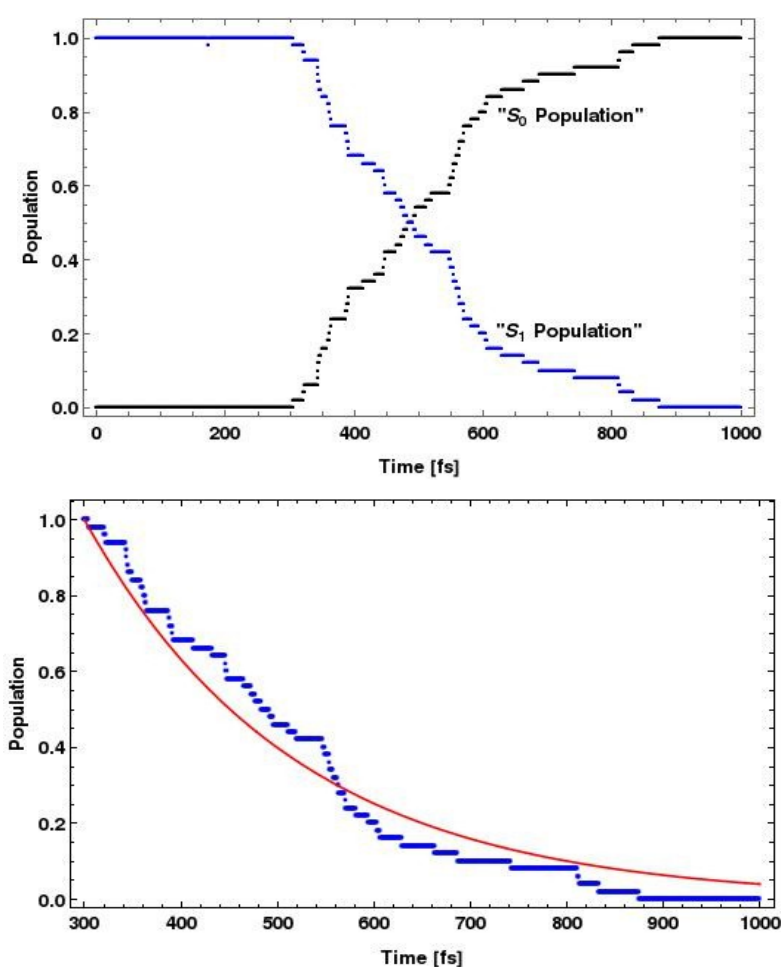


Figure S6. Assumed population decay of the S_1 state (blue) of **1** and the exponential fit (red).

In the case of **2**, S_1 population essentially does not change (≈ 1) during the simulation time of 1 ps, except for a single trajectory reaching the crossing with the ground state (figure S7). The crossing geometry resembles the optimized MECP (see figure 1 in the main text).

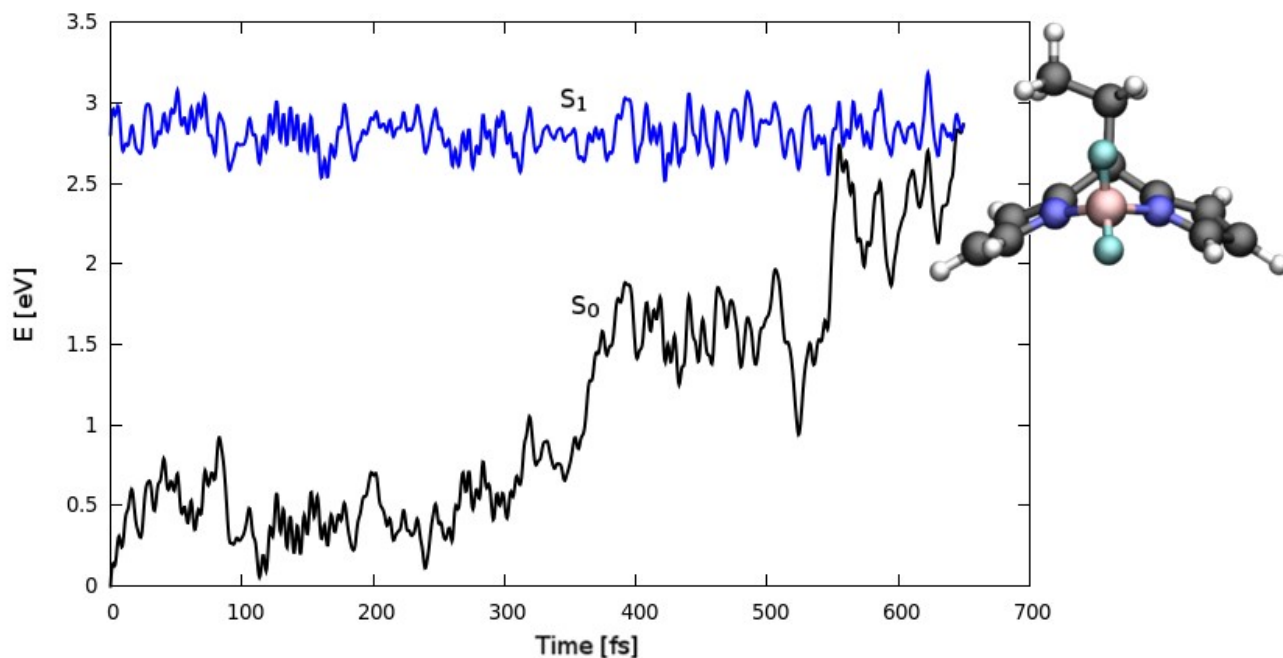


Figure S7. Potential energies of the S_1 and S_0 states for the trajectory of **2** reaching the S_1/S_0 crossing. The molecular geometry at the crossing is depicted. All the energies are relative to the initial (0 fs) S_0 energy. ADC(2)/def2-SVP level was used.

5. Solvent effects

Cosmo model

The conductor-like screening model (COSMO^[1]) computations have been performed with the Turbomole 6.5^[2] program package. The vertical excitations for the first excited state in the tetrahydrofuran (THF) solvent were computed at the ADC(2)/def2-SVP level (the ground state reference treated at the MP2 level; resolution of identity approximation is employed). The dielectric constant of $\epsilon=7.58$ and the refractive index of $n=1.4072$ are used. The parameters for the closed cavity construction were set to their default values ($nppa=1082$, $nspa=92$, $disex=10.00$, $rsolv=\min(\text{rad}(h))$). To construct the cavity, the optimized atomic radii were taken from the Turbomole library.

Both equilibrium and non-equilibrium solvation limits were considered, depending on whether only electronic degrees of freedom of the solvent molecules are adapted to the excited state (non-equilibrium case), or both electronic and nuclear degrees of freedom adapt (equilibrium case).^[3] Both solvation models have their limitations, but provide a consistent picture when compared to the gas phase profiles of **1** and **2** (figure S8). Except for the small energy shifts, there are no qualitative differences from the

gas phase predictions. In case of **2** the crossing region is even less energetically accessible, which agrees well with its emissive behavior. Note that geometry optimizations are currently not available with COSMO solvation and the molecular geometries from the gas phase were used. For the solvent with low dielectric constant excited state structures are expected to be similar to the gas phase ones. Indeed, it was shown that sophisticated solvent model provides similar excited state structures of BODIPY as in the gas phase (at the TDDFT level).^[4]

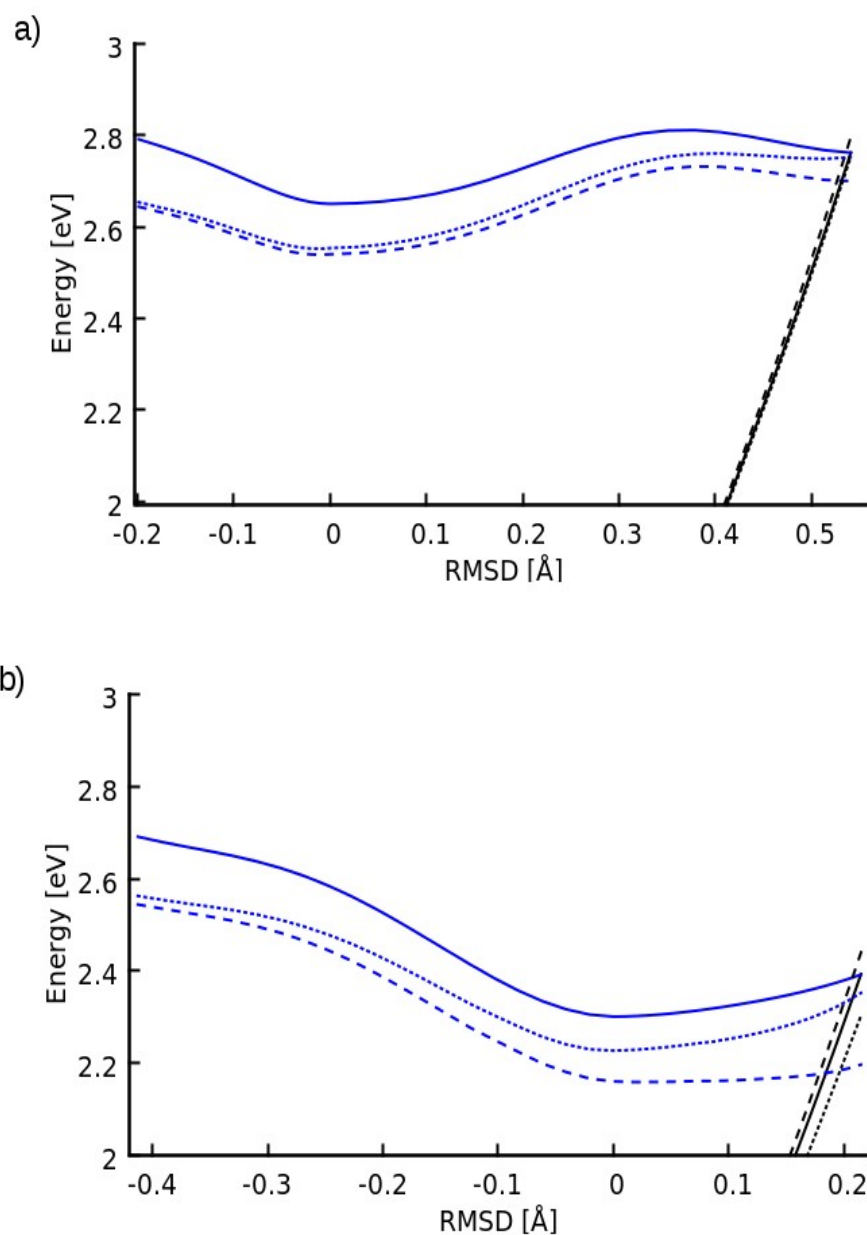


Figure S8. S₁ state energy profiles (in eV) of a) **1** and b) **2** in the gas phase (full lines), non-equilibrium solvation (dotted) and equilibrium solvation (dashed). In all cases the S₀ minimum energy was set to zero. ADC(2)/def2-SVP + COSMO level was used.

QM/MM model

The substituted BODIPY molecules were enclosed in a spherical cluster of 200 tetrahydrofuran (THF) molecules, constructed with the Packmol program package.^[5] The radius of the sphere (18.84 Å) was determined by classical ground state dynamics in the isothermal-isobaric ensemble (NPT, 1 atm, 300 K), using the Tinker 7.1 program package.^[6] All the interatomic potential parameters for THF, including the van der Waals parameters and the effective charges, were taken from the CHARMM general force field (CgenFF),^[7] while the parameters for BODIPY were taken from ref. [8]. The density of THF in the so constructed cluster (880.1 g·L⁻¹) was found to be consistent with the experimental value of 882.7 g·L⁻¹ (1 atm, 298.15 K).^[9]

To perform the mixed quantum mechanical and molecular mechanical (QM/MM) adiabatic dynamics the system was split in two distinct regions: the first containing BODIPY alone (QM region), while the second included all solvent molecules (MM region). QM region was described at PBE0/def2-SVP level for ground state simulations and ADC(2)/def2-SVP (using resolution of identity) for excited state simulations. The solvent was treated as an electrostatic embedding given by spatially localized point-charges. The energies and gradients were computed using the Turbomole 6.5 package^[2], while the MM region was treated using Tinker.^[6] The computation of hybrid energies and gradients, as well as the integration of the equations of motion was performed by the Newton-X 1.4.1 suite of programs^[10]. The file `hybrid_prep_turbomole.pl` was modified to allow QM/MM with ADC(2).

The initial conditions for the excited states dynamics were sampled from the 10 ps ground-state trajectory in the canonical ensemble (NVT, 300K, Andersen thermostat^[11] with collision frequency 0.1 fs⁻¹; nuclear time step of 1 fs). The system was thermalized for 5 ps and the initial conditions for excited state simulations were selected in steps of 0.5 ps from the remaining 5 ps of trajectory. 10 trajectories for each compound (**1** and **2**) were propagated in the first singlet excited state (S₁) for a total time of 1 ps with a nuclear time step of 0.5 fs. The excited states simulations were performed in the microcanonical ensemble (NVE).

However, the total time of 1 ps turned out to be too short for excited state dynamics, which may be attributed to solvent drag which slows down the BODIPY dynamics (compared to the gas phase). We notice that significant numerical problems were encountered during the QM/MM simulations (lack of convergence in ground and excited state) which, along with the huge computational cost, prevented us from extending the dynamics to the longer timescales. Figure S9 shows the time evolution of S₁ – S₀ energy gaps for solvated **1** and **2**.

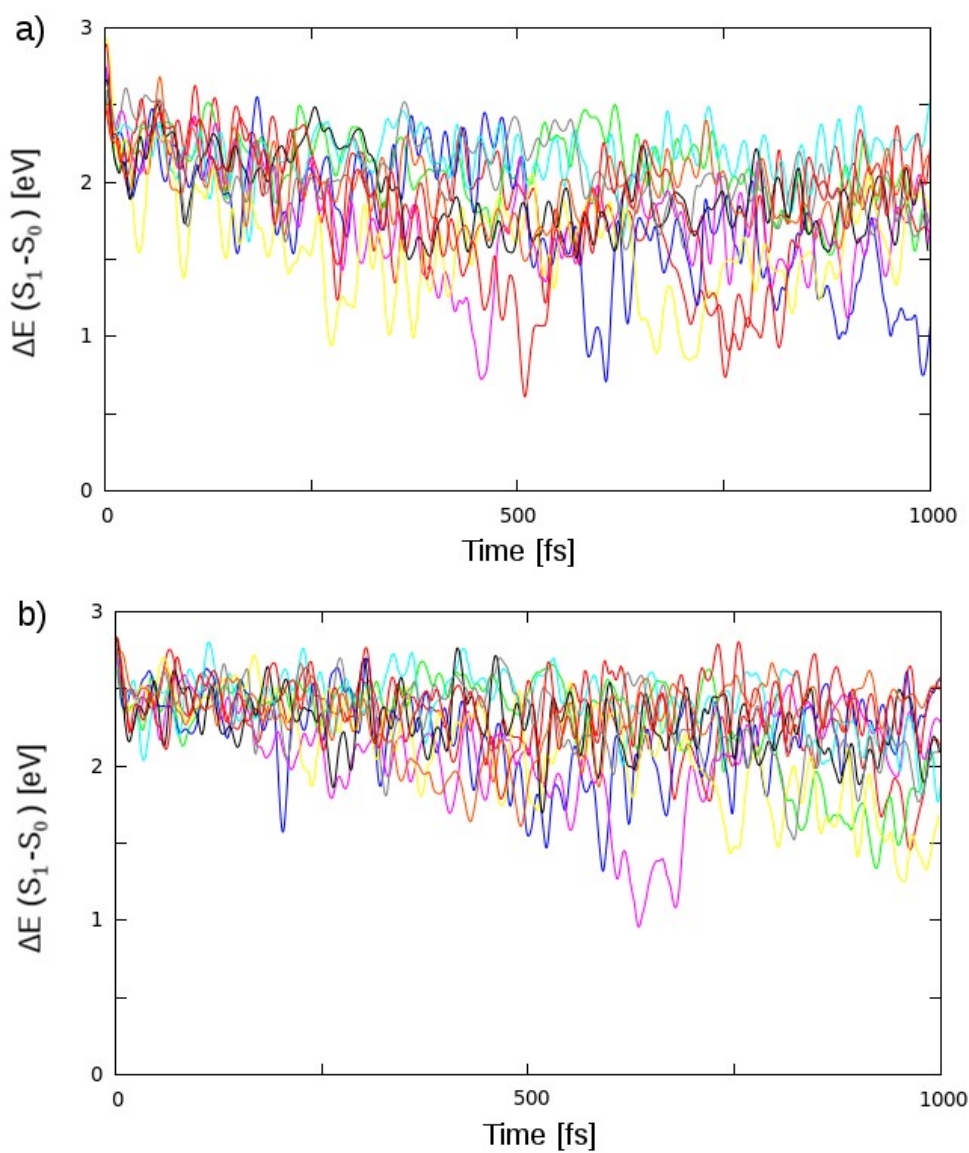


Figure S9. Time evolution of $S_1 - S_0$ energy gaps for 10 QM/MM trajectories of a) **1** and b) **2**. For computational details see the text.

6. References

- [1] A. Klamt and G. Schüürmann, *J. Chem. Soc., Perkin Trans. 2*, 1993, 799.
- [2] F. Furche, R. Ahlrichs, C. Hättig, W. Klopper, M. Sierka and F. Weigend, *WIREs Comput. Mol. Sci.*, 2014, **4**, 91.
- [3] B. Lunkenheimer and A. Köhn, *J. Chem. Theory Comput.*, 2013, **9**, 977.
- [4] D. Jacquemin, S. Chibani, B. Le Guennic and B. Menucci, *J. Phys. Chem. A*, 2014, **118**, 5343.
- [5] L. Martínez, R. Andrade, E. G. Birgin and J. M. Martínez, *J. Comput. Chem.*, 2009, **30**, 2157.
- [6] P. Ren and J. W. Ponder, *J. Phys. Chem. B*, 2003, **107**, 5933.
- [7] (a) K. Vanommeslaeghe and A. D. MacKerell Jr., *J. Chem. Inf. Model.*, 2012, **52**, 3144; (b) K. Vanommeslaeghe, E. Prabhu Raman and A. D. MacKerell Jr., *J. Chem. Inf. Model.*, 2012, **52**, 3155.
- [8] K. C. Song, P. W. Livanec, J. B. Klauda, K. Kuczera, R. C. Dunn and W. Im, *J. Phys. Chem. B*, 2011, **115**, 6157.
- [9] U. Domanska, *J. Chem. Thermodyn.*, 1994, **26**, 1241.
- [10] M. Barbatti, M. Ruckebauer, F. Plasser, J. Pittner, G. Granucci, M. Persico and H. Lischka, *WIREs Comput. Mol. Sci.*, 2014, **4**, 26.
- [11] H. C. Andersen, *J. Chem. Phys.*, 1980, **72**, 2384.